Lawrence Berkeley National Laboratory
Recent Work

Title

INTERDIFFUSION AND MOVING BOUNDARIES IN NiO-CaO AND NiO-MgO SINGLE CRYSTAL COUPLES

Permalink

https://escholarship.org/uc/item/18t5w6q0

Authors

Appel, Marvin
Pask, Joseph A.

Publication Date

1969-10-01

UCRL-18258 Rev.
Preprint

ey. 2

INTERDIFFUSION AND MOVING BOUNDARIES IN
NiO-CaO AND NiO-MgO SINGLE CRYSTAL COUPLES

Marvin Appel and Joseph A. Pask

October 1969

LAWRENCE RADIATION LABORATORY
UNIVERSITY of CALIFORNIA BERKELEY

UCRL-18258 Rev.

DISCLAIMER

Submitted to Journal of the
American Ceramic Society

UNIVERSITY OF CALIFORNIA

Lawrence Radiation Laboratory
Berkeley, California

AEC Contract No. W-7405-eng-48

INTERDIFFUSION AND MOVING BOUNDARIES

IN NiO-CaO and NiO-MgO SINGLE CRYSTAL COUPLES

Marvin Appel and Joseph A. Pask

October 1969

INTERDIFFUSION AND MOVING BOUNDARIES
IN NiO-CaO AND NiO-MgO SINGLE CRYSTAL COUPLES

Marvin Appel and Joseph A. Pask

Inorganic Materials Research Division, Lawrence Radiation Laboratory,
and Department of Materials Science and Engineering,
College of Engineering, University of California,
Berkeley, California

ABSTRACT

October 1969

For single crystal NiO-CaO and NiO-MgO diffusion anneals in air in
the temperature range 1300-1600°C, the diffusivity was found to be ex-
ponentially dependent on the Ni concentration. Diffusion proceeded more
rapidly in the NiO-rich phase resulting in movement of the phase boundary
between the diffusing crystals and growth of the NiO at the expense of
the other crystal. If the two crystals were of different crystallo-
graphic orientation, the orientation of the volume swept out transformed
to that of the growing crystal. The chemical diffusivities for NiO-CaO
interdiffusion were found to be

$$\widetilde{D}_{NiO} = 0.231 \begin{smallmatrix} +.395 \\ -.145 \end{smallmatrix} \exp \left(- \frac{72,090 \pm 3380}{RT} \right) \ cm^2/sec$$

$$\widetilde{D}_{CaO} = 13.9 \begin{smallmatrix} +162 \\ -12.7 \end{smallmatrix} \exp \left(- \frac{93,800 \pm 8630}{RT} \right) \ cm^2/sec$$

Current theoretical and experimental attacks on the nature of Darken's analysis of a moving phase boundary are discussed as is its inapplicability to ionic systems with rigid anion lattices.

I. INTRODUCTION

Interdiffusion of cations in stoichiometric and non-stoichiometric

oxides may give rise to phase boundary motion and crystallographic re-

orientation. These phenomena have practical applications to the under-

standing of grain growth and sintering.

NiO, CaO and MgO provide good materials for such a study since

single crystals are available. Their crystal structures are variants

of the NaCl structure. Mitoff[1] has shown that NiO is non-stoichiometric

in air. There is a finite concentration of Ni^{+3} proportional to $(P_{O_2})^{1/6}$

and equal to 4×10^{-4} atoms per ion pair at 1400°C. The maintenance of

electrovalent neutrality requires that one cation lattice vacancy exists

for every two trivalent nickel ions present. CaO and MgO are stoichio-

metric.

Diffusion in ionic systems has been discussed extensively in the

literature.[2-6] Diffusion in these oxides is dependent upon the presence

of vacancies since the activation energies for other mechanisms--ring,

interstitial, etc.--are too high. Vacancy sites are formed as thermally-

created Schottky defects or by the presence of trivalent impurities or

trivalent nickel ions. The activation energies for the formation of

Frenkel defects in NiO, CaO, and MgO are very high, so that the Frenkel

defect concentrations are negligible in comparison with the Schottky

defect concentrations.

Wartenberg and Prophet[7] report a complete series of solid solutions

for MgO and NiO for all compositions and temperatures. This analysis is

consistent with Hahn and Muan,[8] who used X-ray diffraction to determine

that NiO-MgO solid solutions are ideal for all compositions at low

pressures of oxygen. The lattice parameters of the pure substances are
4.203 $\overset{o}{A}$ and 4.172 $\overset{o}{A}$ for MgO and NiO, respectively.

Blank and Pask[9] have reviewed the diffusion studies in the NiO-MgO
system reported in the literature. They showed experimentally that there
can be a moving boundary in oxide systems, even though a one-for-one
counterdiffusion is necessary across any plane perpendicular to the
direction of diffusion for diffusing species of equivalent charge in
order to maintain a charge balance. For an NiO-MgO diffusion anneal in
air, they found an exponential dependence of the chemical diffusivity
on nickel content and motion of the plane of 25 a/o Ni content. In
vacuum, where there was no concentration-dependence of the chemical
diffusivity, no motion of the 25 a/o Ni plane occurred.

NiO and CaO exhibit a limited solid solubility with no intermediate
compound formation. Tikkanen[10] and more recently Smith et al.[11] have
determined phase diagrams primarily by X-ray diffraction measurements
of lattice parameters. The lattice parameter of CaO is 4.797 $\overset{o}{A}$. The
present diffusion study provides additional information on this phase
diagram. Reports of diffusion studies in the literature in this system
have been limited.

The objective of this study has been to provide a fundamental
understanding of the diffusion characteristics and the phenomenon of
phase boundary motion exhibited in the NiO-MgO and NiO-CaO systems on
annealing in air.

II. EXPERIMENTAL PROCEDURE

Single crystals of MgO, CaO and NiO were used in this study.[*] Their

spectroscopic analyses are listed in Table I. Preliminary diffusion

anneals made with single crystals pressed in powder were abandoned be-

cause they produced erratic results which were attributed to lack of

consistently reliable contacts between the powder and single crystal.

Diffusion couples of NiO-MgO and NiO-CaO were prepared by placing

one crystal on top of another, measuring 0.5-1 cm on a side, with a 210

gram platinum weight load to promote good crystal-crystal contact. The

crystals were offset from one another to aid in the location of the

original phase boundary. This assembly was placed on a platinum foil

in a high-purity Al_2O_3 crucible. Specimens with (100) faces were pre-

pared by cleaving; those with (110) faces, by sawing. In all cases, the

contact surfaces were slightly polished (2 min on a fine diamond lap,

2 min on an extra-fine diamond lap, and 2 min with 1000 grit SiC loose

abrasive in an ethanol slurry) so as to improve contact but not change

the surface characteristics significantly.

Diffusion anneals were made in air at the test temperatures and

times indicated in Table II. The furnace was heated with vertical

$MoSi_2$ hairpins, monitored and controlled by a Leeds and Northrup

Speedomax H recorder-controller. The control thermocouple, Pt vs Pt-10%

Rh, was placed near a hairpin. Another thermocouple placed 1/2" under-

neath the specimen in the center of the hot zone was used to measure

---

[*] Single crystals of MgO and CaO were obtained from Muscle Shoals Electro-
chemical Corporation, P.O. Box 87, Tuscumbia, Alabama; NiO, from
Marubeni-Iida American, Inc., 650 California St., San Francisco, Calif.

the specimen temperature. At no time was it found to deviate by more
than 3°C from the average temperature for the course of the anneal.
The diffusion assembly was introduced into the furnace at temperature,
and the sample always reached thermal equilibrium within 1/2 h. After
the anneal the sample cooled within the furnace with the power off
since the thermal shock associated with immediate extraction frequently
caused the welded crystals to break apart. In all cases, the furnace
temperature dropped below 1000°C within 2-1/2 h and was below 300°C
within 12 h.

Following the diffusion anneal, the welded crystals were sectioned
perpendicular to the original interface with a diamond saw. The sec-
tioned specimen was then polished to optical quality (2 min on a fine
diamond lap, 2 min on an extra-fine diamond lap, 5-10 min on 600 grit
SiC paper, 2 min on 4/0 paper, 4-8 min on a 6 μ diamond lap, and 5 min
with Linde A 0.3 μ Al_2O_3 in an ethanol slurry), and carbon was vacuum-
deposited to improve its surface conductivity in preparation for the
electron microprobe analyzer.

Prior to microprobing, the surface conductivity was further en-
hanced by painting those portions which were not of interest with a
slurry of carbon in ethanol. A Materials Analysis Company Model 400
electron microprobe analyzer was used to determine the concentration vs
distance profiles across the crystal-crystal interfaces.

The nominal beam size was 1 μ, although resolution was probably in
the range of 2-5 μ. In every case, two spectrometers were employed
simultaneously to record the concentrations of both cations at every
point. The specimens were always sufficiently large so that infinite

diffusion theory could be applied in the analysis of the profiles. The

undiffused portions of the specimens served as internal standards

representing spectrometer count rates in the pure oxides.

Laue back-reflection X-ray photographs were taken of all the

specimens to determine the deviation of the microprobe path from the

true normal of the crystal-crystal interface. This deviation resulted

when the specimens were sawed not exactly normal to the interface, and

never exceeded 10°.

Frazer, et al.[12] have written computer programs which correct the

raw microprobe data for dead time, drift, background, absorption, and

fluorescence if any. These programs were modified to suit the Radiation

Laboratory computer facilities and additional programs were written and

incorporated which converted the concentrations into mole fractions,

made the corrections in distance indicated by the Laue photographs, and

used a Cal-Comp plotter to plot automatically the concentration vs dis-

tance profiles.

The concentration-distance coordinates were taken manually directly

from the Cal-Comp plots and punched on computer data cards. Computer

programs were written which used this data to determine the Boltzmann-

Matano interface and the concentration-dependent or independent chemical

diffusion coefficients.

III. MATHEMATICAL ANALYSIS

If the diffusivity is a function of the concentration of the dif-

fusing species, Fick's 2nd law for the one-dimensional case

$$\frac{\partial c}{\partial t} = \frac{\partial}{\partial x} \left(\tilde{D} \frac{\partial c}{\partial x} \right) \tag{1}$$

is an inhomogeneous differential equation. For the case of counter-diffusion in two semi-infinite solids, Matano[13] has modified a solution originally presented by Boltzmann[14] to give the chemical diffusivity $\tilde{D}$ as a function of concentration, distance, and time (c, x, t). The Boltzmann-Matano solution involves the determination of an "interface" across which there has been a zero net flux of atoms of the counter-diffusing species. This defines x = 0 for the solution and is determined by the condition

$$\int_0^{c_0} x\,dc = 0 \text{ for } -\infty < x < \infty. \tag{2}$$

The diffusivity is given by

$$\tilde{D}(c') = -\frac{1}{2t}\left(\frac{dx}{dc}\right)_{c=c'} \int_0^{c'} x\,dc \tag{3}$$

The Boltzmann-Matano solution may not be applied to a system containing two or more phases, since the concentration vs distance profile is discontinuous at the phase boundary or boundaries and the required mathematical operations of integration and differentiation may not be performed. Jost[15] and Heumann[16] have developed qualitative solutions which overcome this difficulty. Appel[17] presented a quantitative solution where, for the two phase case, Eq. (2) becomes

$$\int_0^{c_{1e}} x\,dc + \int_{c_{2e}}^{c_0} x\,dc + (c_{2e} - c_{1e})X = 0 \tag{4}$$

where c_{1e} and c_{2e} are the respective equilibrium concentrations at the phase boundary and X is the distance the boundary has moved. x and X are measured either positive or negative from the x = 0 plane. For a given concentration, c', $\tilde{D}(c')$ is given by Eq. (3) for the region to the left of the discontinuity, and

$$\tilde{D}(c') = -\frac{1}{2t}\left(\frac{dx}{dc}\right)_{c=c'} \left[\int_0^{c_{1e}} x\,dc + \int_{c_{2e}}^{c'} x\,dc + (c_{2e} - c_{1e})\,X \right] \quad (5)$$

for the region to the right of the discontinuity. In the above expressions, t represents the time of the diffusion anneal.

The chemical diffusivity, $\tilde{D}$, is that one defined by Fick's 1st law

$$J = -\tilde{D}\,\frac{\partial c}{\partial x} \quad (6)$$

where J is the atom flux.

Smigelskas and Kirkendall[18] have shown experimentally that when the diffusivity is a function of concentration, the two counterdiffusing species in a metal-metal couple may move at different speeds, so that the original boundary between them and inert markers lying on the boundary move and no longer coincide with the Boltzmann-Matano interface.

Darken[19] developed a theoretical analysis of the Kirkendall effect which relates $\tilde{D}$ and v, the velocity of the inert markers at a constant composition to the intrinsic diffusivities, D_1 and D_2, of the individual, counterdiffusing species at that composition. The relationships are

$$\tilde{D} = D_1 N_2 + D_2 N_1 \quad (7)$$

$$v = (D_1 - D_2) \frac{\partial N_1}{\partial x} \tag{8}$$

where N_1 and N_2 are the atomic fractions of the respective species, subject to $N_1 + N_2 = 1$. When the controlling physical process involved is diffusion, $c = c(xt^{-1/2})$ and $v = X/2t$.

D_1 and D_2 are related to the tracer diffusivities, the diffusivities of radioactive tracer atoms in matrices of their own species (e.g., radioactive gold in gold), by

$$D_1 = D_1^* \left(1 + \frac{d \ln \gamma_1}{d \ln N_1} \right) \tag{9}$$

where D_1^* is the tracer diffusivity and γ_1 is the activity coefficient of component 1 at the concentration represented by N_1. For ideal solutions, $\gamma_1 = 1$ for all N_1 and $D_1 = D_1^*$; likewise, $D_2 = D_2^*$.

Darken's analysis is phenomenological and does not resort to any discussion of mechanisms. Therefore, it should be applicable to diffusion in any state--gas, liquid, or solid. In experiments involving seven different pairs of binary gas diffusion couples, McCarthy and Mason[20] found that Darken's analysis was not valid. The measured diffusivities were found to be related by equations derived from the kinetic theory of gases,[21,22] which are of a different form than Darken's equations.

Birchenall[23] and Vignes and Birchenall[24] have considered the problem from a fundamental viewpoint and believe Darken's equations to be basically incorrect for oxides also. According to them, there is one,

and only one, independent interdiffusion coefficient, the chemical dif-
fusivity $\tilde{D}$, which completely describes the diffusion. D_1 and D_2 are
essentially meaningless quantities, since there is no physical signifi-
cance attached to a plane of constant composition on which inert markers
lie.

Unfortunately, a kinetic theory of solids does not exist. Shewmon[25]
discusses the various attempts which have been made to test Darken's
analysis in solids. All attempts to date have suffered from very large
experimental errors, and while the results agree with the analysis
within those errors, they are by no means conclusive.

IV. RESULTS AND DISCUSSION

(1) Diffusion Profiles

(A) The NiO-MgO System: Typical profiles for this system are
shown in Fig. 1. They are continuous since there is complete solid
solution. An interface exists because a (110) MgO face was in contact
with a (100) NiO face. Profiles for the same system under identical
conditions but with oriented (100) faces in contact were an exact
duplicate; the crystal-crystal interface, however, disappeared. These
results provide experimental proof that the diffusion rate is independent
of the crystallographic direction in cubic crystals. Nye[26] presents a
theoretical proof.

Each of the profiles, for Ni and Mg, were analyzed independently,
as discussed in Section III, to give $\tilde{D}$. As reported by Blank and Pask,[9]
these diffusivities were always found to vary exponentially with Ni con-
centration. Since the diffusivity is also proportional to the vacancy
concentration, it follows that the vacancy concentration varies

exponentially with total nickel concentration. Similar effects have been observed by Zintl[27] and Werner.[28] Zintl investigated cation lattice vacancies as a function of composition in Co_xO-MgO solid solutions and found that the vacancy concentration varied exponentially with cobalt concentration. Werner measured electrical conductivity in (Cu,Ag)S solid solutions as a function of copper composition. (Cu,Ag)S is a pure ionic conductor where electrical conductivity occurs by vacancy diffusion of the cations. The vacancy concentration depends on the fraction of Cu^{+2} present. He found that the electrical conductivity varied exponentially with copper concentration; which is to say, the vacancy concentration varied exponentially with copper concentration. These three effects are all manifestations of the same phenomenon. A small addition of the potentially-oxidizable ion present in the lattice will result in greater oxidation and formation of vacancies. Furthermore, since $Ni_{\square} \ \alpha \ e^{B[Ni]} \ \alpha \ e^{-\Delta H}f/RT$, the heat of formation of a vacancy, ΔH_f, will decrease linearly with increasing nickel concentration. An ordered array of vacancies will have a lower energy per vacancy than will an isolated vacancy in the ordered crystal lattice. The vacancies interact with one another to lower the total energy of the system.

The total amount of Ni^{+3}, however, is small, the mole fraction being about 10^{-4} or less. This is indicated by the fact that the Ni and Mg profiles are complementary within experimental error. It may also be assumed that the NiO was at thermodynamic equilibrium with respect to its Ni^{+3} concentration throughout the course of the diffusion anneals since Mitoff[1] reports equilibrium with respect to thermal conductivity in times less than 2 h for temperatures in excess of 1300°C.

The $\tilde{D} = Ae^{B[Ni]}$ dependence was evaluated for three NiO-MgO diffu-
sion couples—two at 1346°C for 173.26 h and one at 1342°C for 236:54 h.
A and B were determined for each couple by a least-squares analysis and
then a weighted average was taken of all three with weights inversely
proportional to the individual variances. It was found that

$$\tilde{D} = 7.19 \times 10^{-12} \exp \{(4.31 \pm 0.11) \ [Ni]\} \ cm^2/sec \qquad (10)$$

where [Ni] is expressed in atomic fraction Ni. In an analysis of just
the nickel profiles in MgO single crystals, Blank and Pask[9] found that

$$\tilde{D} = 7.6 \times 10^{-12} \exp \{5.37 \ [Ni]\} \ cm^2/sec \qquad (11)$$

at 1370°C and that B was constant between 1200 and 1400°C. They also
found that the activation energy for diffusion was 45.5 kcal/mol and
remained constant for all compositions.

From Eq. (1) it is seen that $\tilde{D}$ varies between 7.19×10^{-12} and
$4.87 \times 10^{-11} \ cm^2/sec$ in going from pure MgO to pure NiO. This variation
is less than an order of magnitude, so an average value of $\tilde{D}$ could be
calculated. It was found to be $4.07 \times 10^{-11} \ cm^2/sec$.

Choi and Moore[29] found that radioactive Ni^{+2} tracer diffusion in
NiO was described by the equation $D = 1.83 \times 10^{-3} \exp \left(-\dfrac{45,600}{RT}\right)$, so
that $D_{1345°C} = 1.21 \times 10^{-9} \ cm^2/sec$. For radioactive Mg^{+2} tracer diffu-
sion in MgO, Lindner and Parfitt[30] found $D = 0.249 \exp \left(\dfrac{-79,000}{RT}\right)$, so
that $D_{1345°C} = 4.86 \times 10^{-12}$. It is seen that the average value obtained
in this study for the bulk interdiffusion lies between these two, as

expected. Wuensch and Vasilos[31] measured Ni^{+2} tracer diffusion in MgO

and determined $D = 1.80 \times 10^{-5} \exp(-\frac{48,500}{RT}) = 4.84 \times 10^{-12}$ at 1345°C

which is in good agreement with Lindner and Parfitt's determination for

Mg^{+2} in MgO. In Blank and Pask's experiments, single crystals of MgO

were embedded in NiO powder and the concentration profiles were measured

only for Ni in the single crystal. Their determination, $\tilde{D} = 1.70 \times 10^{-5}$

$\exp(-\frac{42,800}{RT}) = 2.70 \times 10^{-11}$ at 1345°C is slightly lower than that of

this study, 4.07×10^{-11} cm^2/sec, as would be expected if the higher

diffusivity regions in the NiO were not included.

The diffusion in these couples was of the extrinsic type since the

MgO single crystals contained 0.015% Al as an impurity. The number of

lattice cation vacancies from this source is greater than the number

created thermally.[9]

(B) The NiO-CaO System: Typical profiles for this system are

shown in Fig. 2. Discontinuities exist at the crystal interface because

of limited solid solutions. The finite resolution of the electron micro-

probe beam caused the sharp discontinuities at the phase boundary to

appear experimentally as non-vertical lines. The effect of this on

calculations involving these results is negligible, since the deviations

from straight, vertical lines are sufficiently small.

Each of the profiles, for Ni and Ca, was analyzed independently.

The low mutual solubilities of NiO and CaO prevented a determination of

the constants in the $\tilde{D} = Ae^{B[Ni]}$ dependence, but since the concentration

span was never very great, averages could be taken for the respective

diffusivities in each phase. Furthermore, since the mole fraction of

Ni^{+3} (and thus lattice vacancies) is small, the diffusion profiles for

Ni and Ca are mirror images reflected about the Ni = Ca = 0.25 atomic
fraction composition line. $\tilde{D}$ for Ni should then equal $\tilde{D}$ for Ca at each
composition plane. The experimental data were averaged accordingly in
each matrix.

Table II lists the experimentally-determined average diffusivities.
These values were then fitted to equations of the form $\tilde{D} = D_o e^{-\Delta H/RT}$
(Fig. 3) to obtain the respective pre-exponential terms and activation
energies. The results of a least-square analysis are shown in Table III;
the indicated respective limits represent one standard deviation of the
calculated values.

The coefficients for the CaO matrix are for intrinsic diffusion
rather than extrinsic diffusion. There are more thermally created
lattice vacancies (Schottky defects) than there are vacancies due to the
presence of impurities of valence greater than +2. Consequently, the
concentration of vacancies is temperature-dependent and is part of ΔH,
rather than being a temperature-independent component of D_o. For intrin-
sic diffusion,

$$\Delta H = \Delta H_m + \Delta H_s/2 \tag{12}$$

where ΔH_m is the heat of motion and ΔH_s is the heat of formation of a
Schottky defect.

Lindner[32] has determined the intrinsic tracer diffusion of Ca^{+2}
in CaO to be $D = 0.4 \exp(-\frac{81,000}{RT})$ while Gupta and Weirick[33] have
determined the extrinsic diffusion to be $D = 1.95 \times 10^{-7} \exp(-\frac{34,020}{RT})$
so that $\Delta H_s = 94,000$ cal/mol = 4.07 ev/defect for pure CaO. On

theoretical grounds, Yamashita and Kurosawa[34] have predicted Schottky

defect heats of formation of 3-5 ev in CaO. The agreement is good. For

an assumed heat of formation of 4 ev, the equilibrium concentration of

cation vacancies at the lowest temperature of the anneals, 1342°C, is

given by

$$N_{Ca} = \left(e^{-4\times23,100/1.99\times1615}\right)^{1/2} = 5.4 \times 10^{-7} \tag{13}$$

where N_{Ca} is the mole fraction of calcium ion lattice vacancies. The

spectroscopic analyses listed in Table I do not show the presence of

any trivalent or quadrivalent impurities with greater concentrations.

The activation energy for interdiffusion in the CaO matrix,

93.80 ± 8.63 kcal/mol, is in fair agreement with the self-diffusivity for

Ca^{+2} in CaO, 81.0 kcal/mol. No data exists for the activation energy for

self-diffusion of Ni^{+2} in NiO in air but it should be less, since there

are always excess cation vacancies available due to the presence of Ni^{+3}.

The activation energy for self-diffusion of Ni^{+2} in NiO in air is

probably very close to the activation energy for interdiffusion determined

in this study, 72.09 ± 3.38 kcal/mole.

(2) Moving Phase Boundaries

    (A) The NiO-MgO System: A photomicrograph of a polished cross-

section of the NiO-MgO diffusion couple with composition profile of

Fig. 1, but with oriented (100) faces in contact, is shown in Fig. 4.

The original boundary is obliterated except for a line of elongated

pores arising from the original imperfect matching of the two crystals.

This line of pores is identifiable as the site of the original boundary

by its coincidence with the portion of the edge of the MgO crystal

which was offset and because the cation concentration at this line is

identical to that at the Boltzmann-Matano interface (30.4 a/o Ni and

19.8 a/o Mg, which adds to 50 a/o total cation concentration within

experimental error) as determined by the computer analysis.

Figure 5 is a photomicrograph of the couple with a NiO (100) face

in contact with a (110) MgO face whose diffusion profiles are also

represented by Fig. 1. In this case the crystal offset is reversed

and the phase boundary has clearly moved into the MgO crystal. To

determine what happens to the crystallographic orientation of the volume

swept out by the moving boundary, another diffusion anneal of a similar

couple was made at 1342°C for 236:54 h. The boundary moved 51.4 μ into

the MgO. The crystals broke apart at this interface. Laue back-

reflection X-ray diffraction photographs of the new surfaces showed that

the crystallographic orientation of the material swept out by the

boundary changed from (110) to (100).

This movement is not generated by differences in surface energies

at the interface. On the basis of thermal stabilities (at 1700°K,

Coughlin[35] reports that ΔF for MgO is -91.3 kcal/mol and for NiO, -20.0

kcal/mol; also NiO decomposes rapidly in vacuum at temperatures greater

than 1400°C) NiO would be expected to have a lower surface free energy

than MgO. Then, the usual driving force for grain growth would have

caused the boundary to move into the NiO, instead of into the MgO as was

found here.

(B) The NiO-CaO System: A photomicrograph of a polished cross-
section of the NiO-CaO couple, whose diffusion profiles are represented
by Fig. 2, is shown in Fig. 6. The phase boundary remains because of
limited solid solubility, but it has moved into the CaO as indicated by
its curvature at the offset. The black area is due to material lost
during polishing; it can thus be seen that the tip of the curved inter-
face coincides with the offset CaO surface which also coincides with the
Boltzmann-Matano interface.

In any diffusion-controlled process, $c = c(xt^{-1/2})$ only, so that at
the Boltzmann-Matano interface, where $x = 0$ for all t, the concentration
is invariant. Table II lists the independently-determined concentrations
of each cation at the respective Boltzmann-Matano interfaces for each
diffusion anneal. Within experimental error, the sum of the cation con-
centrations is 0.500 mole fraction; also the concentrations are constant
at a given temperature.

The experimentally determined average velocities of phase boundary
motion are listed in Table II and plotted as a function of the inverse
absolute temperature in Fig. 7. A least squares analysis gives the
equation listed in the figure. The activation energy of 61 ± 9 kcal/mol
is close to the value of 72 ± 3 kcal/mol determined for interdiffusion
in the NiO matrix. This agreement suggests that the boundary motion is
primarily governed by the diffusion in the matrix that has the higher
diffusivities.

The instantaneous velocity of the boundary at a given time can be
mathematically calculated by equating the difference in the diffusion
fluxes in the two phases at the interface to the rate of transfer of

material to the growing phase.

(C) Mechanisms: Diffusion experiments with oxide systems have indicated that essentially a rigid anion lattice is maintained. Oishi and Kingery[36] and O'Keefe and Moore[37] have shown that the oxygen diffusivities in MgO and NiO, respectively, are many orders of magnitude lower than the diffusivities of the corresponding cations. Also, Carter[38] has shown with the aid of markers that the oxygen anion lattices are rigid during interdiffusion in the $MgO-Al_2O_3$ and $MgO-Fe_2O_3$ systems. Since there is no net flux of oxygen atoms, a one-for-one exchange of cations of equivalent charge must occur at each plane normal to the diffusion direction in order to maintain a charge balance. The original interface then becomes the mass balance plane and corresponds to the Boltzmann-Matano interface which is indicated in Figs. 1 and 2. The requirement for maintenance of electroneutrality means that at each plane $D(Ni) = D(Ca)$ or $D(Ni) = D(Mg)$. The diffusion rate at each plane, however, may be different due to any variations in vacancy concentrations that may exist.

The observed moving boundary, thus, is not a Kirkendall marker in the sense that the term is used by Kirkendall[18] and Darken,[19] for its movement does not result from an unequal counterdiffusion at a given plane. Darken's analysis therefore cannot be applied to ionic systems of this type, since the species do not counterdiffuse independently of one another. Equations (7) and (8) consequently are inoperative since in this case $D_1 = D_2 = \tilde{D}$.

It is possible, however, to apply a Darken's analysis approach using Eqs. (7) and (8) to calculate the pseudo intrinsic diffusivities

D(Ni) and D(Ca) or D(Mg) if the assumption is made that D(Ni) is not
equal to D(Ca) or D(Mg) at a given point. Such calculations were made
using the $\tilde{D}$ and v data obtained in this study.[39] These calculations
indicated that in regions where the nickel concentration was large, D(Ni)
was large and negative. Thus, although mathematical treatment is possible,
the values obtained are meaningless on the basis of the proposed
mechanism or model wherein D(Ni) must equal D(Ca) or D(Mg) at a given
concentration.

The driving force for the phase boundary motion arises from the
difference in the chemical diffusivities in the portions of the phases
adjoining the boundary; in this case diffusion in the NiO-rich phase is
more rapid than either in the MgO-rich or CaO-rich phases. The MgO or
CaO concentration on the NiO side of the boundary thus tends to deplete
more quickly than the NiO concentration on the MgO or CaO side of the
boundary. This situation leads to a continuous reaction at the interface
in order to maintain equilibrium compositions resulting in the movement
of the boundary into the MgO or CaO phase. Without a net oxygen flux,
this movement involves a rearrangement and a transfer of oxygen anions
to the growing phase at the boundary. This rearrangement or reaction
occurs more rapidly than the diffusion; for otherwise, the (100) vs (100)
and (100) vs (110) diffusion profiles in the NiO-MgO couples would not
be identical and continuous, and the compositions at the phase boundary
in the NiO-CaO couples would not be constant with time at a given
temperature.

(3) NiO-CaO Phase Diagram

Short and Roy[40] have shown that diffusion data can be used to yield information on equilibrium phase diagrams. The concentrations in the respective phases at the phase boundary represent the equilibrium solubilities for the annealing temperature when the reactions are faster than the diffusivities. The equilibrium molar solubilities of CaO in NiO and NiO in CaO found for the air diffusion anneals in this study are listed in Table II and shown in Fig. 8. The figure shows the superimposed phase diagrams for the NiO-CaO system published by Tikkanen[9] and more recently by Smith et al.[11] The reasons for the lack of agreement between the three studies were not resolved.

V.   CONCLUSIONS

1. In an air diffusion anneal of two semi-infinite solids, NiO and MgO or NiO and CaO, the variable vacancy concentration due to the varying content of Ni^{+3} with varying total NiO content causes the diffusivity to be concentration-dependent. Therefore, diffusion proceeds more rapidly in NiO-rich regions.

2. For NiO-MgO anneals in air, the dependence of the chemical diffusivity is

$$\tilde{D} = 7.19 \times 10^{-12} \exp \left\{ (4.31 \pm 0.11)[Ni] \right\} \quad cm^2/sec \qquad (10)$$

where [Ni] is expressed as atomic fraction Ni. This form of the dependency is due to the exponential dependence of Ni^{+2} vacancy concentration on Ni content, which in turn is due to the lower energy per vacancy when there are many vacancies present in the lattice.

3. The difference in the chemical diffusivities in the phases at the boundary will cause the phase boundary to move into the CaO in an NiO-CaO anneal and into the MgO in an NiO-MgO anneal when the faces originally in contact are of different crystallographic orientation. In the case of NiO-MgO diffusion anneals, no phase boundary exists when like crystallographic orientations are in contact. For an NiO-CaO anneal, the motion of the phase boundary is governed by the equation

$$v = 0.044^{+.651}_{-.041} \exp\left(-\frac{60,910 \pm 9340}{RT}\right) \text{ cm/sec} \qquad (14)$$

This result agrees with the measured activation energy in the NiO matrix indicating that the boundary motion is governed primarily by diffusion in the matrix exhibiting faster diffusivities.

4. When crystals of diverse crystallographic orientations are annealed in contact, the volume swept out by the moving boundary changes its orientation to conform to that of the growing crystal. Grain growth occurs.

5. The observed phase boundary motion is not a Kirkendall effect in the classical sense. In ionic solids with rigid anion lattices, electroneutrality requires that the respective intrinsic diffusivities of the two counterdiffusing cation species be equal at a given plane perpendicular to the direction of diffusion. Darken's analysis cannot be applied to such systems.

ACKNOWLEDGMENTS

11. D. E. Smith, T. Y. Tien, and L. H. Van Vlack, "The System NiO-CaO,"
    J. Am. Ceram. Soc., 52 (9), 459-460 (1969).

12. J. Z. Frazer, et al., "Computer programs EMX and EMX2 for electron
    microprobe data processing," Scripps Institute of Oceanography,
    University of California, San Diego; La Jolla, California.

13. C. Matano, "On the relation between the diffusion coefficients and
    concentrations of solid metals. (The nickel-copper system)."
    Japanese J. Phys., 8 (3), 109-113 (1933).

14. L. Boltzmann, "Zur integration der diffusionsgleichung bei variabeln
    diffusionscoefficienten," Ann. Phys., 53, 959-964 (1894).

15. W. Jost, "Bemerkung zur mathematischen behandlung komplizierter
    diffusionsprobleme," Z. Phys., 127, 163-167 (1950).

16. T. Heumann, "Zur berechnung von diffusionskoeffizienten bei ein -
    und mehrphasiger diffusion in festen legierungen," Z. Phys. Chem.,
    201, 168-189 (1952).

17. M. Appel, "Solution for Fick's 2nd law with variable diffusivity
    in a multi-phase system," Scripta Met., 2, 217-222 (1968).

18. A. D. Smigelskas and E. O. Kirkendall, "Zinc diffusion in alpha
    brass," Trans. AIME, 171, 130-142 (1947), as discussed in Ref. 4,
    Chap. 4.

19. L. S. Darken, "Diffusion, mobility and their interrelation through
    free energy in binary metallic systems," Trans. AIME 175, 184-201
    (1948).

20. K. P. McCarthy and E. A. Mason, "Kirkendall effect in gaseous
    diffusion," Physics of Fluids, 3 (6), 908-922 (1960).

21(a). C. F. Curtiss and J. O. Hirschfelder, J. Chem. Phys., 17 (6),
        550-555 (1949), as quoted in Ref. 27.

   (b). C. F. Curtiss and J. O. Hirschfelder, "The theory of flame propa-
        gation," J. Chem. Phys., 17 (11), 1076-1081 (1949), as quoted in
        Ref. 27.

22. J. O. Hirschfelder, C. F. Curtiss, and R. B. Bird, Molecular Theory
     of Gases and Liquids (John Wiley and Sons, New York, 1954), as
     quoted in Ref. 27.

23. C. E. Birchenall, private communication.

24. A Vignes and C. E. Birchenall, "The phenomenological theory of
     diffusion and the Kirkendall effect," unpublished.

25. Reference 4, Chap. 4.

26. J. F. Nye, Physical Properties of Crystals (Clarendon Press,
     Oxford, 1957).

27. G. Zintl, "Untersuchungen über das metalldefizit in den systemen
     kobaltoxid-magnesiumoxid und kobaltoxid-nickeloxid," Z. Phys. chem.
     48, 340-358 (1966).

28. A. Werner, "Untersuchungen am system kupfer-silber-schwefel,"
     Z. Phys. Chem., 47, 267-285 (1965).

29. J. S. Choi and W. J. Moore, "Diffusion of nickel in single crystals
     of nickel oxide," J. Phys. Chem., 66, 1308-1311 (1962).

30. R. Lindner and G. D. Parfitt, "Diffusion of radioactive magnesium
     in magnesium oxide crystals," J. Chem. Phys., 26 (1), 182-185
     (1957).

31. B. J. Wuensch and T. Vasilos, "Diffusion of transition metal ions
     in single-crystal MgO," J. Chem. Phys., 36 (11), 2917-2922 (1962).

32. R. Lindner, "Studies on solid state reactions with radiotracers,"
    J. Chem. Phys., 23, 410-411 (1955).

33. Y. P. Gupta and L. J. Weirick, "Self-diffusion of calcium in single
    crystal calcium oxide," J. Phys. Chem. solids, 28, 811-821 (1967).

34. J. Yamashita and T. Kurosawa, "Formation energy of lattice defect
    in simple oxide crystals," J. Phys. Soc. Japan, 9, 944-953 (1954).

35. J. P. Coughlin, "Contributions to the data on theoretical metallurgy.
    XII. Heats and free energies of formation of inorganic oxides,"
    U. S. Bureau of Mines Bull. 542, 1954.

36. Y. Oishi and W. D. Kingery, "Oxygen diffusion in periclase crystals,"
    J. Chem. Phys., 33, (3), 905-906 (1960).

37. M. O'Keefe and W. J. Moore, "Diffusion of oxygen in single crystals
    of nickel oxide," J. Phys. Chem., 65, 1438-1439 (1961).

38. R. E. Carter, "Mechanism of solid-state reaction between magnesium
    oxide and aluminum oxide and between magnesium oxide and ferric
    oxide," J. Am. Ceram. Soc., 44 (3), 116-120 (1961).

39. M. Appel, "Interdiffusion in NiO, CaO, and MgO Single Crystals,"
    (Ph.D. Thesis), UCRL-18258, 57p (1968).

40. J. M. Short and R. Roy, "Use of interdiffusion to determine
    crystalline solubility in alkali halide systems," J. Am. Ceram.
    Soc. 47 (3), 149-151 (1954).

Table I. Spectroscopic Analyses

Impurity (Reported as w/o oxide)	MgO	CaO	NiO
Mg	P.C.	0.04	0.001
Al	0.015	<0.002	<0.003
Si	Undetected	<0.002	<0.005
Ca	0.04	P.C.	0.001
Ti	Not analyzed	<0.005	<0.003
Cr	0.001	<0.0005	<0.001
Mn	Undetected	<0.0005	<0.001
Fe	0.008	<0.003	<0.005
Co	Not analyzed	<0.003	<0.01
Ni	<0.002	<0.001	P.C.
Cu	0.001	0.001	<0.0005
Sr	Not analyzed	0.015	Undetected
Sn	Not analyzed	<0.005	<0.01
Ba	Not analyzed	0.002	<0.001
W	Not analyzed	Undetected	Undetected

The analyses were performed by the American Spectrographic Laboratories, Inc., 557 Minna Street, San Francisco, California.

Table II. Data for Interfaces and Average Diffusion Coefficients in
NiO–CaO and NiO–MgO Systems in Air

Temp °C	Time hrs	Mole Fractions at Boltzmann–Matano Interfaces		Mole Percent at Phase Boundary		Phase Boundary Velocity $\times 10^{10}$ cm/sec	Average Diffusion Coefficients in	
		Ca	Ni	CaO in NiO	NiO in CaO		NiO Matrix	CaO Matrix
1346	173:26	.0402	.4608	7.4	2.6	2.92	3.97×10^{-11}	7.13×10^{-12}
1352	122:35	.0372	.4621	6.7	6.6	3.22	5.34×10^{-11}	1.91×10^{-12}
1352	251:59	.0412	.4590	6.7	6.6	2.96	5.14×10^{-11}	2.65×10^{-12}
1410	97:57	.0613	.4376	8.7	7.9	4.47	7.77×10^{-11}	6.63×10^{-12}
1420	170:42	.0456	.4531	9.0	8.2	7.16	1.32×10^{-10}	7.41×10^{-12}
1423	266:37	.0485	.4516	9.1	8.3	5.08	1.06×10^{-10}	2.29×10^{-11}
1481	169:10	.0569	.4421	12	5.0	12.11	2.44×10^{-10}	1.95×10^{-11}
1481	169:10	.0507	.4493	11	6.6	5.05	2.33×10^{-10}	2.37×10^{-11}
1524	47:48	.0663	.4355	14	6.4	34.12	3.93×10^{-10}	4.97×10^{-11}
1527	171:53	.0504	.4507	16	6.5	12.49	3.55×10^{-10}	7.98×10^{-11}
1527	123:03	.0629	.4373	14	5.4	23.82	4.83×10^{-10}	7.27×10^{-11}
		Mg	Ni				NiO Matrix	MgO Matrix
1346	173:26	.1872	.3156					
1346	173:26	.1984	.3040				4.07×10^{-11}	
1342	236:54	.1961	.3034					

Table III. D_o and ΔH for the Diffusivities for the
NiO-CaO System

|	D_o	ΔH(kcal/mol)
NiO Matrix	$0.230\ ^{+.395}_{-.145}$	72.09 ± 3.38
CaO Matrix	$13.9\ ^{+162}_{-12.7}$	93.80 ± 8.63

FIGURE CAPTIONS

Fig. 1. Diffusion profiles for (100) NiO face in contact with (110)
MgO face.

Fig. 2. Diffusion profiles for NiO-CaO couple with (100) faces in contact.

Fig. 3. Chemical diffusivities in NiO-CaO system: averages for respective
matrices.

Fig. 4. Micrograph of NiO-MgO diffusion couple with (100) faces in
contact. The leftmost line of pores corresponds to the original
interface. (X100)

Fig. 5. Micrograph of NiO-MgO diffusion couple with (100) NiO face in
contact with (110) MgO face. (X100)

Fig. 6. Micrograph of NiO-CaO diffusion couple with (100) faces in
contact. (X100)

Fig. 7. Velocity of phase boundary motion in NiO-CaO diffusion couples
with (100) faces in contact.

Fig. 8. NiO-CaO phase diagram.

Fig. 1

XBL 686-923

Fig. 2

XBL 686-921

$$\widetilde{D}_{NiO} = 0.230^{+.395}_{-.145}\exp\left(-\frac{72,090\pm3380}{RT}\right)$$

$$\widetilde{D}_{CoO} = 13.9^{+162}_{-127}\exp\left(-\frac{93,800\pm8630}{RT}\right)$$
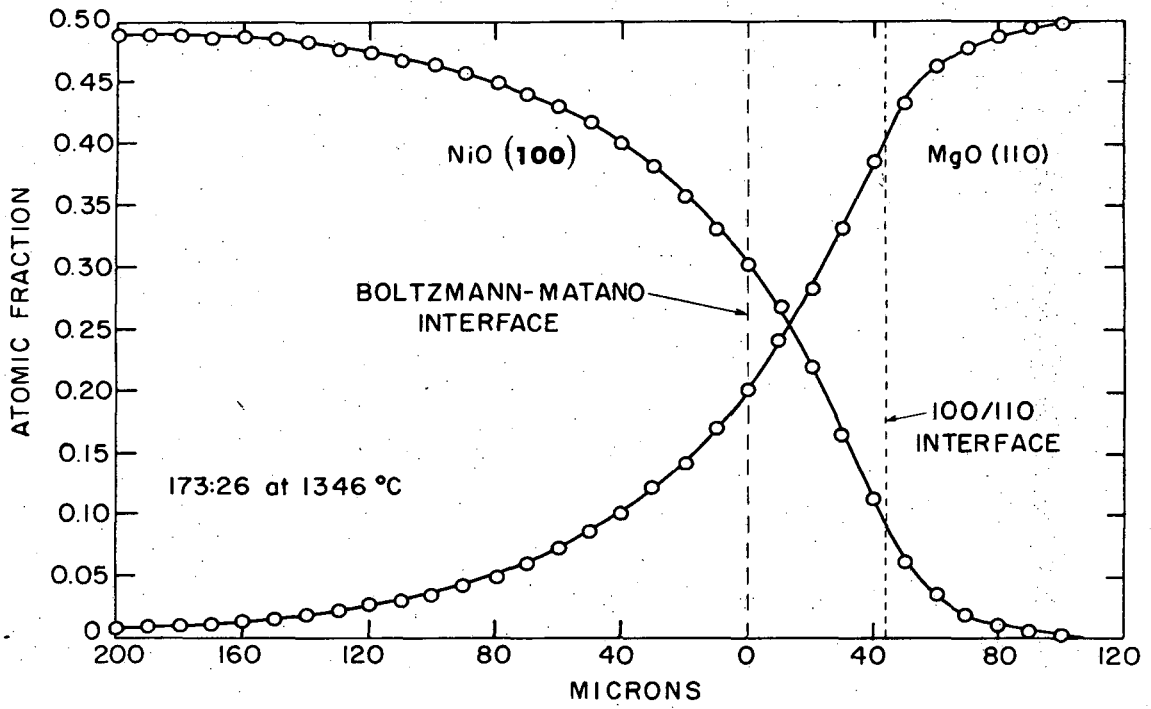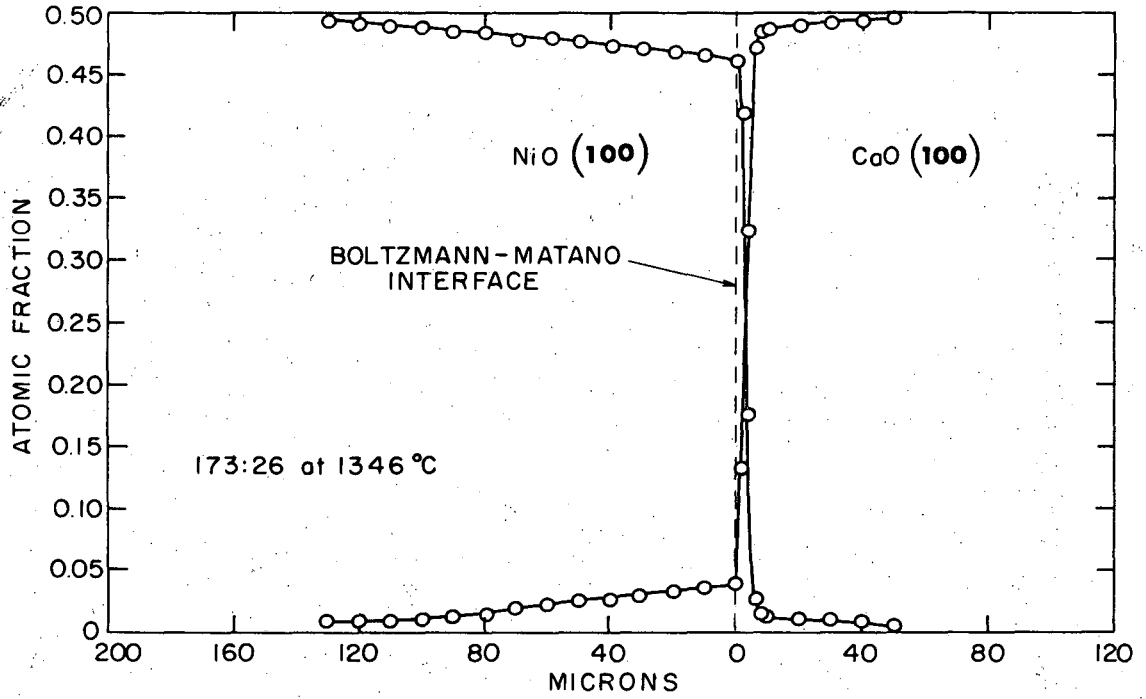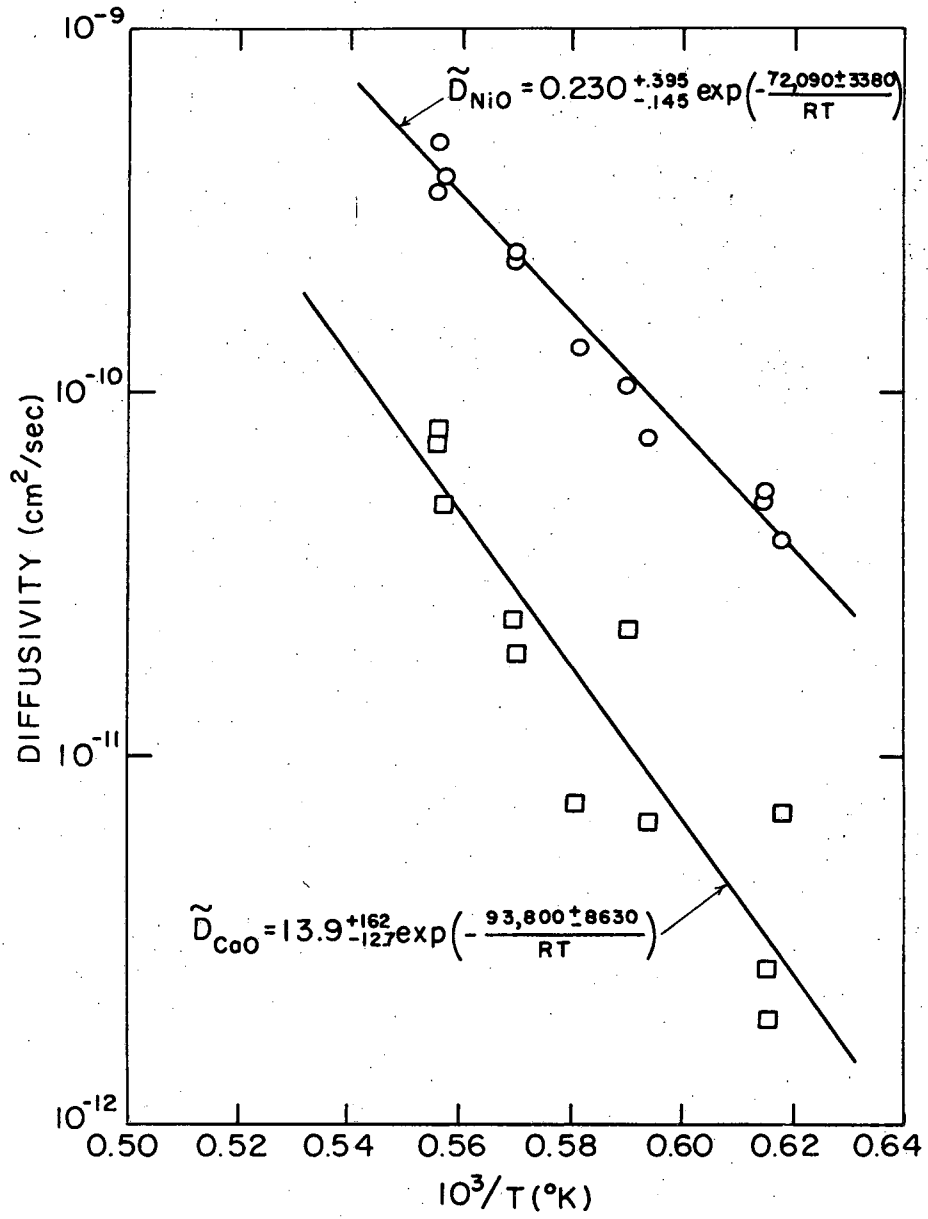
Fig. 3
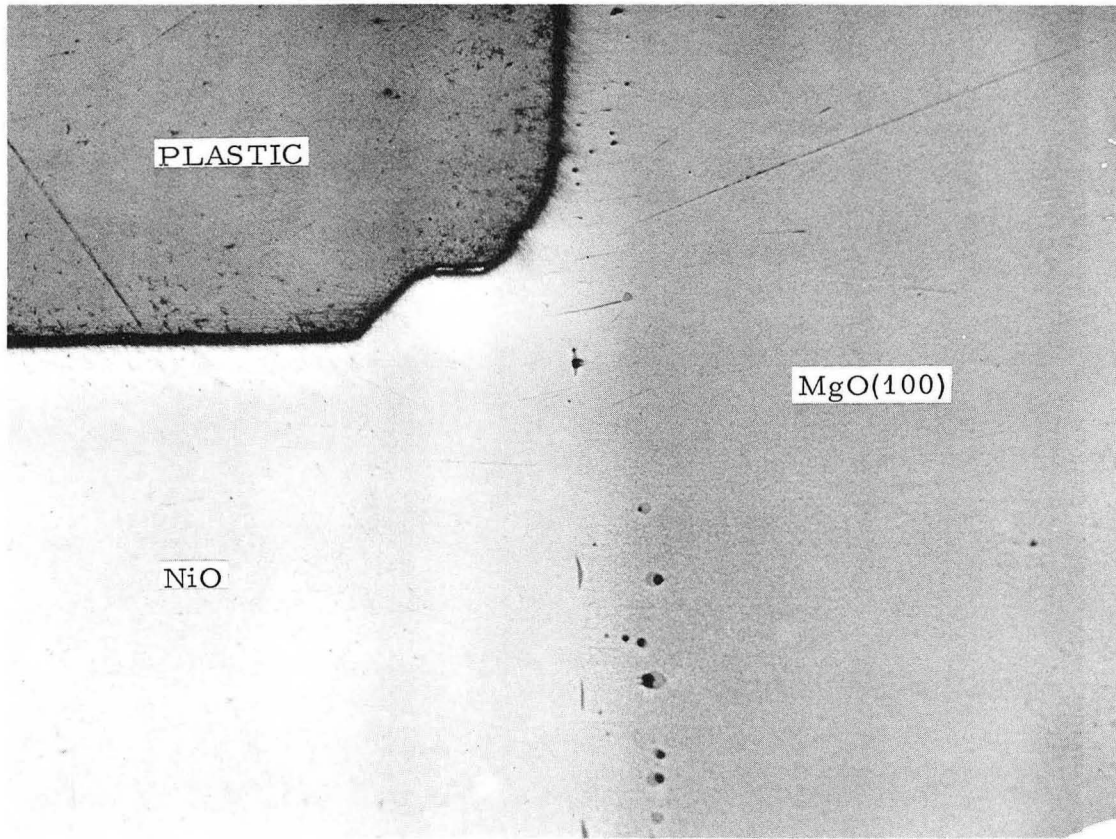
XBL 686-926

XBB 687-3314-A

Fig. 4
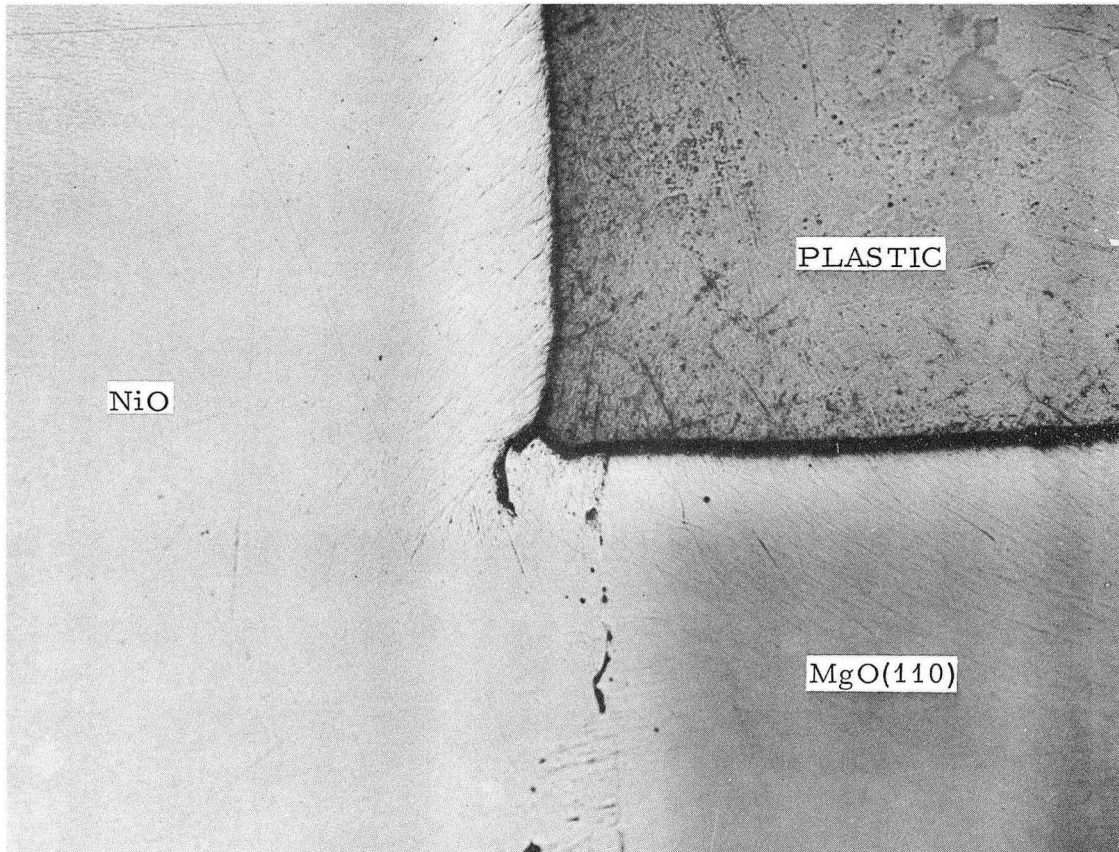
XBB 687-3313-A

Fig. 5

XBB 687-3315-A

Fig. 6

Fig. 7

Fig. 8

XBL 699-5673